Desalination and Water Treatment
www.deswater.com

doi: 10.5004/dwt.2018.22703

122 (2018) 112–123
August

Application of green coagulants on paint industry effluent – a coagulation–flocculation kinetic study

S. Vishali[a,*], R. Karthikeyan[b]

[a]*Department of Chemical Engineering, SRM University, Kattankulathur – 603 203, Tamil Nadu, India, Tel. +91 9443883562; email: meet.vishali@gmail.com*
[b]*Anjalai Ammal Mahalingham Engineering College, Thanjavur – 614 403, Tamil Nadu, India, Tel. +91 9940561915; email: drrkarthi@yahoo.com*

Received 28 February 2018; Accepted 25 June 2018

ABSTRACT

The behavior of green, eco-friendly coagulants, derived from *Strychnos potatorum*, *Cactus opuntia*, *Moringa oleifera*, *Cyamopsis tetragonolobus* and *Portunus sanguinolentus* was evaluated and optimized for the removal of color and turbidity from simulated paint industry effluent (SPE). A series of bench-scale flocculation experiments were conducted in jar test apparatus to examine the optimal dose of coagulant, at different initial pH and initial concentration of the effluent. The eluent type and concentration were varied, to extract the maximum amount of active coagulant compounds viz, proteins (from *S. potatorum, M. oleifera*), cellulose (from *C. opuntia*), chitosan (from *P. sanguinolentus*), polysaccharides (from *C. tetragonolobus*) and to attain the maximum removal efficiency. The obtained optimized conditions from the SPE were applied for the treatment of real paint industry effluent. All the five coagulants exhibited the maximum removal efficiency at the actual pH of the effluent itself. The coagulation kinetic study suggests the order of kinetics, and the model parameters were obtained from the linear equations. The time evolution pattern of formation of monomers, dimmers and trimmers was evaluated. The comparisons of the green coagulants with chemical coagulants have also been studied.

Keywords: Paint effluent; Green coagulants; Turbidity; Kinetics; Cluster size distribution

1. Introduction

The growth in the construction business aided by the easy availability of housing loans is the prime driving force for the growth of the decorative paint industry. The industrial paint sector is witnessing a 50% increase in revenue, mainly due to a 10% rise in the manufacture of automobiles [1]. The Indian paint industry produces around 940 million liters of paint and is valued at approximately USD 2 billion. At present, India has more than 20,000 outlets in operation, which is probably the highest for any country. 30% of the paint industry's revenue is derived from the sale of industrial paints [2]. Paint manufacturing is a branch of the chemical industry and it is a mixture of pigment, binder, solvent and additives. The cleaning of vessels and various unit operations is the main source of the wastewater (80%) generated in the paint industry [3]. Paint wastewater contains high concentrations of suspended solids, pigments, color, heavy metals, oil and grease. The presence of chemical components in the paint effluent can irritate eyes, skin and lungs, and cause nausea, headache. It can also contribute to human health risks such as Alzheimer's diseases, respiratory problems; muscle weakness, liver and kidney damage and cancer, and the spoil of aquatic system was attributed due to the direct release of this

* Corresponding author.

Presented at the 3rd International Conference on Recent Advancements in Chemical, Environmental and Energy Engineering, 15–16 February, Chennai, India, 2018.

effluent. To respect the environment and the law, the generated wastewater has to be treated before disposal [4].

Researchers have reported the treatment of paint industry wastewater by various methods such as physical–chemical treatment [5], bio-oxidation [6], biological treatment [7], active sludge treatment [8], microfiltration [9], coagulation–flocculation processes [10], Fenton oxidation [11], adsorption [12], electrochemical oxidation [13] and electro-coagulation [4]. Among these, coagulation–flocculation has historically attracted considerable attention for its high removal efficiency. It was concluded as that a well-suited method for the paint effluent treatment is coagulation [14] due to the enormous amount of suspended solids.

Researchers have developed several natural and synthetic adsorbents with a modified structure based on nanotechnology, co-polymerization techniques in the decolorization of synthetic aqueous dye solutions such as fast green dye [15], coomassie brilliant blue [16], methylene blue dye [17], malachite green [18], methyl orange, Congo red [19] dyes and rose Bengal dye [20]. But the decolorization of paint effluent was not addressed much.

The disadvantages associated with using chemical coagulants are ineffectiveness in low temperature water, relatively high procurement cost, adverse effects on human health, and production of large volumes of sludge and their significant effect on pH of treated water. The presence of toxic pollutants in the sludge formed by chemical coagulant leads to Alzheimer's disease in humans, which initiated the development of the alternate coagulant [21].

The effective treatment process depends not only on the toxin expulsion capacity of the coagulant but also on the wealth of the material reachable. So the coagulant might be (i) a residue from industry and/or (ii) accessible bounty in environment [22]. It is, in this way, attractive to supplant these chemical coagulants with plant-based coagulants to counter the disadvantages mentioned above.

The following are the advantages of the natural coagulants: material is apparent, it is cost effective, unlikely to alter the pH of treated water, and is highly biodegradable. In the age of climate change, depletion of the earth's natural resources and widespread environmental degradation, usage of green coagulants for water and effluent treatment is a global sustainable development initiative [23]. The treated wastewater can be effective, recycled and reused, within the plant as a coolant, diluent or a component of low-cost paint and for effective water management.

Researchers have spotted several plant types such as *Phaseolus vulgaris,* gum arabic*, Moringa oleifera, Ipomoea dasysperma, Strychnos potatorum, Cactus opuntia and Prosopis juliflora* and as coagulants in the water and wastewater treatment [24].

S. potatorum, known as a clearing nut tree, grows in southern and central parts of India, Sri Lanka and Burma. Sanskrit writings from India report that the seeds were used to clarify turbid surface water over 4,000 years ago [24]. By reviewing the literature, it was observed that *S. potatorum* seeds were used as a natural coagulant to clarify turbid water [25,26] and as an adsorbent to remove the heavy metals from aqueous solution [27,28].

C. opuntia is a cheap and abundantly available plant. The main constituent of the cactus cladode is a heteropolysaccharide with a molecular weight of 23–300 × 10^4 g/mol. Nopal cladode has been utilized in the turbidity removal of the synthetic water as a coagulant [29]. It was used as a coagulant in the treatment of cosmetic industry wastewater [30], toxic textile dyes [31], and the poultry slaughterhouse wastewater [32].

M. oleifera is a non-toxic (at low concentrations) tropical plant found throughout India, Asia, sub-Saharan Africa and Latin America. It is suggested that its active coagulating agents are dimeric cationic proteins with molecular mass of 12–14 kDa, isoelectric point (pI) between 10 and 11, and its main coagulation mechanism is adsorption and charge neutralization. Researchers have reported the coagulation ability of *M. oleifera* in the removal of heavy metals [33], treatment on tannery effluent and turbidity from water [34].

Guar gum, which structurally comprises a straight chain of D-mannose with a D-galactose side chain on approximately every other mannose unit, has a molecular weight of the order of 220,000. As a result of its wide range of properties, guar gum is the most extensively used gum, both in food and industrial applications. It is nonionic and hence an effective flocculent over a wide range of pH and ionic strengths. The broad vibration due to the presence of intermolecular hydrogen bonding/O–H bond stretching is around 3,340 cm^{-1} in the case of the water eluted sample > 1 M NaCl eluted sample > 1 M KCl eluted sample [35]. The influence of the eluent type and concentration on color and turbidity removal efficiencies was acknowledged through the intensity of a peak in FTIR. In recent days, researchers are testing guar gum as a natural coagulant in the potable water treatment [36], treatment of tannery wastewater [37] and in the removal of COD from wastewater [38].

Seafood processing factory ended with millions of tons of crab shells annually worldwide. Land filling of waste disposal is obscure, because of environmental concern and more expenses. Finding the new utility of the material could become an alternative result and develop gain to the industries [39]. The presence of chitosan, in the crab and shrimp shells was evaluated. Chitosan is a high-molecular weight linear cationic polymer applied for heavy metal adsorption, drinking water and effluent treatment [35,40,41]. 465 g of chitosan can be gained from about 100 g of crab shell powder [42].

2. Materials and methods

2.1. Paint industry effluent

2.1.1. Simulated paint industry effluent

Analytical grade chemicals were used in the experiments. Simulated paint industry effluent (SPE) was made by blending different proportions of commercially available white primer and acrylic-based blue colorant (5% (v/v)) [43]. Five different samples were produced and named as sample numbers 1–5 (Table 1).

2.1.2. Real paint industry effluent

The real (water sourced) paint industry effluent (RPE) was collected from paint industry located in Chennai, South India. The physico–chemical properties of both SPE and RPE are listed in Table 2.

Table 1
Concentration of SPE (made up to 1,000 mL)

Sample number	White primer (mL)	Blue colorant (mL)	Initial COD (mg/L)
1	48	2	3,100
2	46	4	4,224
3	44	6	5,650
4	42	8	6,258
5	40	10	7,693

Table 2
Physico-chemical characteristics of paint effluent

Parameters	Concentration (except for pH, color and turbidity, viscosity)	
	Real wastewater (RPE)	Simulated wastewater (SPE)
pH at 25°C	7.03	7.6
Color	Dark black	Blue
Total dissolved solids, mg/L	1,234	304
Total suspended solids, mg/L	300	6,880
Oil and grease, mg/L	15	19
Sulfate as SO_4, mg/L	115	24
Chemical oxygen demand (COD), mg/L	1,760	7,693
Biochemical oxygen demand, mg/L (3 d incubated at 27°C)	880	2,648
Turbidity, NTU	198.5	7,760
Viscosity, kg/m.sec	0.015	0.0144

2.2. Coagulant

2.2.1. Plant based

The seeds of *S. potatorum, M. oleifera*, *C. tetragonolobus* (guar gum) and the pods of *C. opuntia* were collected from Thirumayam, a rural area of Pudukottai district, South India. The seeds were washed thoroughly with distilled water, sun dried for 48 h, powdered and sieved through 0.5 mm sieve. The thorns present in the pods of *C. opuntia* were completely removed before washing thoroughly with distilled water, after which the pods were sliced into small pieces, and dried in a convection oven at 100°C for 1 h with periodical supervision. The dried material was powdered using a conventional mixer and sieved through a 0.5 mm sieve (Figs. 1(a)–(d)).

2.2.2. Animal based

Clean *P. sanguinolentus* (crab) shells sourced from Jegathapattinam situated on the eastern coast were purchased from the local seafood market of Pudukottai, South India. The shells of three red-spotted crab were cleaned completely with distilled water to separate the smooth tissues within, sun dried for 2 h, crushed using a standard kitchen blender and the powder was screened through a 0.5 mm sieve (Fig. 1(e)).

2.3. Equipment

A conventional six stirrer arrangement jar test apparatus (Deep Vision, India) with a base floc illuminator with an inbuilt speed regulator (up to 300 rpm) and timer was used for the batch mode of the coagulation procedure. The length and breadth of stirrer paddles are 8 cm and 22 cm, respectively (Fig. 2).

2.4. Preparation of coagulant extract

To extract the active components from the natural coagulants, the known amount of the prepared coagulant powder was suspended in 100 mL of solvent termed as eluent. The suspension was stirred for 15 min to excerpt the active compounds. After 15 min of settling span, the clarified liquid was collected from the top, called as eluate and was used as a coagulant for further studies. The presence of active compounds which are responsible for the coagulation was tabulated in Table 3 for all the five coagulants.

2.5. Experimental setup

2.5.1. Coagulation–flocculation–sedimentation

To execute the treatment process, known volume of coagulant eluate was added in a liter of SPE. The jar test apparatus (Fig. 2) was used for the coagulation study and agitated at a rapid mixing of 200 rpm for 2 min and slow mixing at 80 rpm for 20 min followed by the settling period span of 60 min. After this, 50 mL of clarified sample was collected to measure the residual color and turbidity. The experimental procedure was repeated to study the effect of operational variables viz, eluent type, eluent concentration, coagulant dose, coagulant–eluate volume, initial pH and initial effluent concentration.

All the experiments were rerun minimum thrice for consistency and the mean was taken for the outcome. The plot was made for the mean value with the reproducibility greater than 98%. At the end of the setting period, the amount of sludge formed was noted. The optimized conditions to treat a liter of SPE (Table 4) and the maximum removal efficiencies obtained at the optimized conditions (Table 5) are consolidated.

The optimized treatment conditions obtained from the SPE were applied on the treatment of the RPE collected from the paint factory by following the same experimental procedure. The results and the kinetics are discussed in the present study.

2.6. Parameters evaluation

The coagulation ability of the natural coagulants was analyzed in terms of residual color and turbidity. Using the standard methods, the parameters given in Table 2 was measured [42]. At λ_{max} 612 nm (SPE) and 285 nm (RPE) in a SL 218 double UV visible spectrophotometer (Elico, India) the

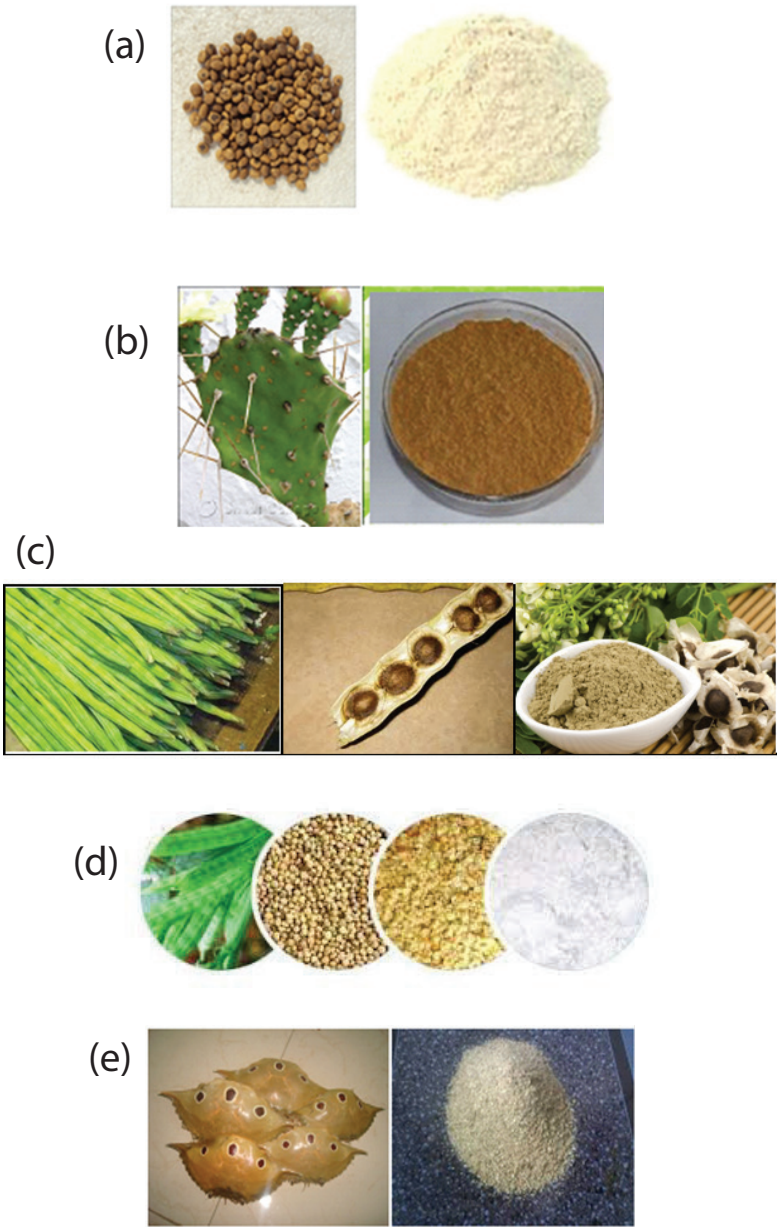

Fig. 1. (a) Seeds and powder of *S. potatorum*, (b) *C. opuntia* pods and powder, seeds and powder of (c) *M. oleifera*, seeds and powder of (d) *C. tetragonolobus*, and (e) *P. sanguinolentus* (crab) shells and powder.

Fig. 2. Jar test apparatus.

residual color was measured. Turbidity was measured using a digital nephelo-turbidity meter 132 (Elico, India) and it was expressed in nephelometric turbidity units (NTU). pH is adjusted using a digital pH meter MKVI (Elico, India).

3. Modeling of coagulation kinetics

For a wastewater treatment plant to be economical, one of the most important parameters is equilibrium time. Taking RPE as the target of treatment and several coagulants as the subject of investigation, the effect of the settling period on the percentage removal of pollutants such as color and turbidity was evaluated. It became evident that a longer settling time

Table 3
Presence of active compounds in natural coagulants

Coagulant	Active compounds	Method	Reference
S. potatorum	Protein	SDS-PAGE and Bradford method	[50]
C. opuntia	Cellulose	Glucose solution	[51]
M. oleifera	Protein	SDS-PAGE and Bradford method	[34]
C. tetragonolobus	Polysaccharides	FTIR spectrum	[53]
P. sanguinolentus	Chitosan	FTIR spectrum	[52]

Table 4
Optimized values of operational parameters to treat a liter of SPE

Coagulant	Eluent and concentration	Dose and eluate volume	Initial pH	Initial concentration	Reference
S. potatorum	3 N NaCl	2 g, 100 mL	7	7,693 mg/L Sample 5	[50]
C. opuntia	3 N NaCl	3 g, 100 mL	7		[51]
M. oleifera	1 N NaCl	3 g, 80 mL	8		–
C. tetragonolobus	1 N KCl	5 g, 100 mL	8		[53]
P. sanguinolentus	3 N NaCl	3 g, 100 mL	9		[52]

Table 5
Comparison of the treatment efficiency of the green coagulants on SPE and RPE under optimum conditions

Coagulants	SPE		RPE	
	Color removal %	Turbidity removal %	Color removal %	Turbidity removal %
S. potatorum	98.21	85.57	84.70	89.57
C. opuntia	88.37	82.60	64.82	79.78
M. oleifera	95.2	88.6	88.77	92.00
C. tetragonolobus	85.2	84.7	86.37	88.72
P. sanguinolentus	92.3	86.65	86.81	89.57

effected greater pollutant removal, and that a 60 min contact period was sufficient to reach equilibrium. Data gathered from this part of the investigation were utilized to understand kinetics models.

Kinetic sorption data using natural green coagulants were useful in comprehending the dynamic process of pollutant removal from RPE in terms of the rate constant. The parameters of coagulant kinetics make significant contributions by providing valuable information necessary for designing and modeling the sorption process [43]. In turn, sorption kinetics is vital for enumerating the coagulant–pollutant interaction as well as system conditions, and can be applied successfully in the control of water pollution. Rapid kinetics is one of the most crucial considerations for removal processes, and depends upon mechanism and reaction rates. Solute uptake rate determines the residence time required for completion of the sorption reaction, and can be evolved from kinetic analysis [44]. Information on the kinetics of pollutant uptake is essential for deciding optimum operating conditions for a full-scale batch process [45].

Several kinetic models were therefore tried and tested during the course of the present study. Selection of the most suitable model was based on (a) comparison of the experimental and simulated data, and (b) evaluation of the correlation between coagulation properties and model theory [46].

An understanding of the adsorption mechanism, and identification of potential rate-controlling processes such as chemical reaction, diffusion control and mass transport, was gained by the use of kinetic models to test the experimental data. The models taken for the investigation included first-order model, second-order model, pseudo-first order, Elovich, Bangham, intraparticle diffusion and Avrami (Table 6). Microsoft Excel spreadsheets were used to compute the values of experimentally determined ($q_{e,\exp}$), calculated ($q_{e,\mathrm{cal}}$), and correlation coefficient (R^2), along with the kinetic rate constants [47].

The cluster size distribution for the coagulation–flocculation as a function of time can be generally termed as:

$$N_m(t) = 4N_o^{\,m}(kt)^{m-1}(2 + kN_o t)^{-(m+1)} \quad (1)$$

for monomer m = 1, dimmer m = 2, and trimmer m = 3, respectively.

4. Results and discussion

4.1. RPE treatment

The RPE was treated using the optimized treatment conditions procured from the SPE for all the five green

Table 6
Linear form of kinetic models

Models	Linear equation
First-order kinetic model	$\ln (C_o/C) = k_1 t$
Pseudo-first-order kinetic model	$\log(q_e - q_t) = \log q_e - \frac{k'}{2.303} t$
Elovich	$q_t = \frac{1}{\beta_E} \ln(\propto_E \beta_E) + \frac{1}{\beta_E} \ln t$
Bangham model	$\log q_t = \log k_B + \frac{1}{m_B} \log t$
Intraparticle diffusion model	$q_t = k_{id} t^{0.5} + I$
Avrami model	$\ln\left(-\ln\left(1 - \frac{q_t}{q_e}\right)\right) = \ln(k_{Av}) + m_{AV} \ln t$

coagulants. The treatment expertise was graded using color and turbidity and shown in Figs. 3(a) and (b) and listed in Table 5.

In the course of settling span, the color removal efficiency was swelled up for all the green coagulants till the end of the 60th min. The maximum removal was viewed as 84.70%, 64.82%, 88.77%, 86.37% and 86.81% for *S. potatorum*, *C. opuntia*, *M. oleifera*, *C. tetragonolobus* and *P. sanguinolentus*, respectively.

Akin orientation was noted for the removal of turbidity. The maximal removal efficiency was observed at the end of the 60th min and the values are 89.6%, 79.8%, 92.0%, 88.7% and 89.6% for *S. potatorum*, *C. opuntia*, *M. oleifera*, *C. tetragonolobus* and *P. sanguinolentus*, respectively. The reasons and the discussions behind the influence of the operating variables on removal efficiency were elaborated in detail [48–51].

The treatability of the green coagulants using color and turbidity removal efficiency was compared in Fig. 4. It was noticed that among the five green coagulants *M. oleifera* revealed its maximum capacity in the treatment of RPE, both in color and turbidity removal. The photographs of treated samples using five green coagulants are shown in Fig. 5.

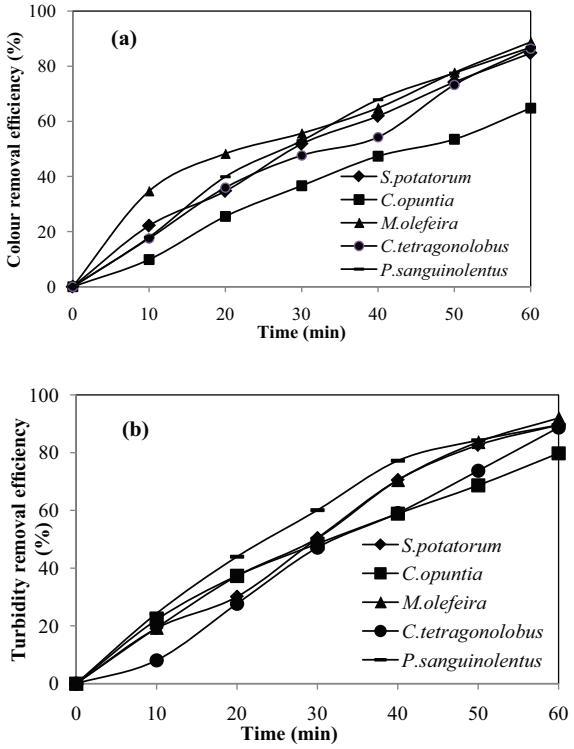

Fig. 3. (a) Color removal efficiency and (b) turbidity removal efficiency.

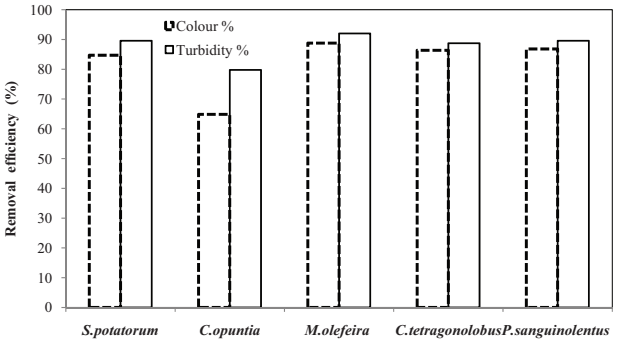

Fig. 4. Comparison of performance of green coagulants.

4.2. Kinetic studies

4.2.1. First order

The residual turbidity (NTU) of the RPE was measured as a function of time and then it was transformed into concentration (mg/L) by multiplying with the factor 2.3 [34]. It was detected that the turbidity concentration was decreased with increase in time. The reason is that, when the reaction is in progress, the number of particles available for the coagulation is reduced.

To study the coagulation kinetics, with time, a physical property which influences the treatment efficiency was also studied, by keeping further parameters viz, pressure drop, temperature, film/pore diffusion as constant. The linear form of first-order equation is given in Table 6. The plots were made between time and $\ln(C_o/C)$ (Fig. 5), the model parameters such as linear regression coefficient (R^2), rate constant k_1 (1/min), $t_{0.5}$ (min), β (m³/kg s), D (kg²/m s), K_{Rc},

Table 7
Model parameters

Parameter	First-order kinetic model	Second-order kinetic model
$t_{0.5}$ (min)	$0.6931/k_1$	$0.6931/k_2$
β (m³/kg s)	$2k_1$	$2k_2$
D (kg²/m s)	$k_B T/\beta$	$k_B T/\beta$
K_{Rc} (1/min)	$4\, k_B T/3\mu$	$4\, k_B T/3\mu$
E	k_1/K_{Rc}	k_2/K_{Rc}

E are tabulated in Tables 7 and 8. In Fig. 6(a), the plots are linear but do not pass through the origin and show a negative intercept, indicating that the process was not in acknowledgement with the experimental values for all the five green coagulants.

Though the linear regression coefficient (R^2) values are greater than 0.9 for all the plots, it can be confirmed only the scope of linearity of the plots.

4.2.2. Pseudo-first-order kinetic model

The parameters of the pseudo-first-order kinetics model (Table 6) calculated from the linear plot of log ($q_e - q_t$) vs. t (Fig. 6(b)) and together with the corresponding correlation coefficients (R^2) are summarized in Table 9. It is evident that in every case, the correlation coefficients for the pseudo-first-order kinetic model ($R^2 > 0.9$), were higher, and that the calculated values of $q_{e,\text{cal}}$ derived from the kinetics model were near the experimental values ($q_{e,\text{exp}}$). This is a clear indication that the pseudo-first-order kinetics model was reliable in its description of the adsorption kinetics mechanism [47]. The findings revealed that pollutant adsorption on natural coagulants was in compliance with the pseudo-first-order mechanism and second, that the chemical sorption process controlled the sorption rate [43].

4.2.3. Elovich model

The Elovich model parameters were evaluated from the slope and intercept of the linear plot of t vs. q_t (Fig. 6(c)). The α_E (mg/min g) is related to the rate of chemisorption (initial adsorption rate) and β_E (g/mg) is related to surface coverage (desorption constant) (Table 6). Interpretations of the Elovich equation are usually connected to the heterogeneous surfaces [48]. The Elovich equation data and the correlation coefficients values obtained, R^2, are listed in Table 9.

The kinetic curve of sorption demonstrated good fitness with the model ($R^2 > 0.95$), thus reinforcing the feasibility of the Elovich model. The Elovich equation does not predict any definite mode of function, but it is useful in describing the phenomenon of adsorption by highly heterogeneous adsorbents [52]. The large values of α_E (>1) elicited in the trial run of this model implied that the model was capable of explaining heterogeneity of surface coagulants; the small values of β_E (<1) indicated non-occurrence of the chemisorption reaction. This means that the model can be safely used for accurate prediction of experimental data. This model supports the hypothesis that the heterogeneous sorption mechanism is probably responsible for pollutant uptake. The experimental results confirmed that the adsorption rate could be maximized under optimal experimental conditions [53].

4.2.4. Bangham model

The application of Bangham's equation (Table 6) to kinetic data served the purpose of checking whether pore diffusion was the only rate-controlling step in the adsorption system or not, where, k_B (mg/g min) and $1/m_B$ are the sorption rate constants (Fig. 6(d)).

Larger values of k_B (>1) under conditions of optimum individual design variable quantities, were indicative of the suitability of material for pollutant removal [53] (Table 9). The graph for each coagulant was found to be linear with good correlation coefficient (>0.9). These findings can be interpreted as follows: the kinetics mechanism confirmed Bangham's equation and therefore the theory that adsorption

Fig. 5. RPE samples after the treatment.

Table 8
Model parameters of First-order kinetic model

First order	*S. potatorum*	*C. opuntia*	*M. oleifera*	*C. tetragonolobus*	*P. sanguinolentus*
R^2	0.957	0.982	0.944	0.916	0.99
k_1 (1/min)	0.038	0.025	0.041	0.034	0.038
$t_{0.5}$ (min)	18.24	27.72	16.90	20.39	18.24
β (m^3/kg s)	0.076	0.05	0.082	0.068	0.076
D (kg^2/m s)	5.505×10^{-20}	8.369×10^{-20}	5.103×10^{-20}	6.15×10^{-20}	5.506×10^{-20}
K_{Rc} (1/min)	3.72×10^{-18}	3.72×10^{-18}	3.72×10^{-18}	3.72×10^{-18}	3.72×10^{-18}
E	1.02×10^{16}	6.72×10^{15}	1.10×10^{16}	9.14×10^{15}	1.02×10^{16}

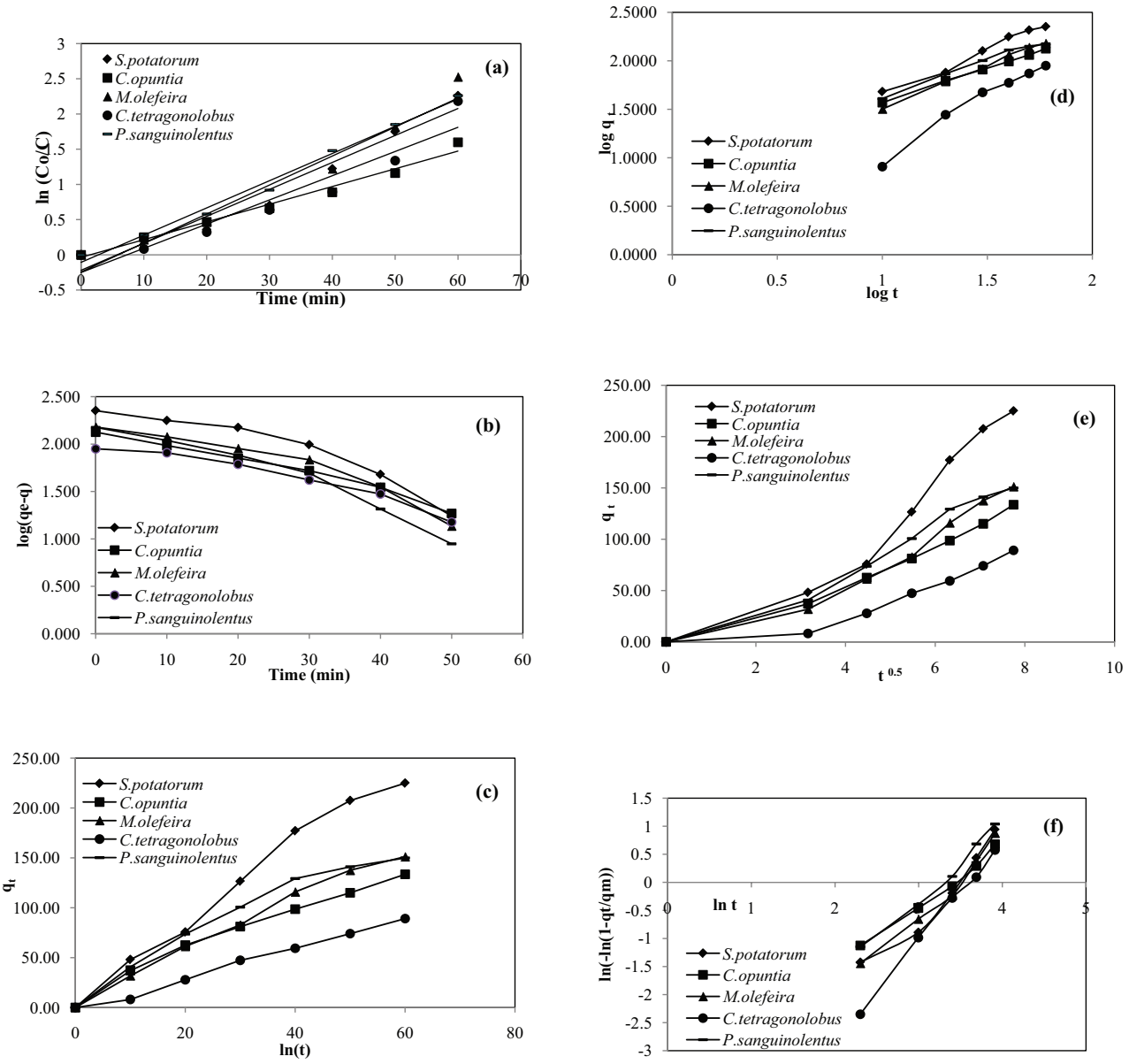

Fig. 6. Kinetic plots of green coagulants. (a) First-order kinetic model, (b) pseudo-first-order kinetic model, (c) Elovich model, (d) Bangham model, (e) intraparticle diffusion model and (f) Avrami model.

of pollutant from RPE onto natural coagulants was pore diffusion controlled.

4.2.5. Intraparticle diffusion model

According to this model (Table 6), a graph plotted with solute adsorbed q_t against the square root of the contact time $t^{0.5}$, should be a straight line passing through the origin when intraparticle diffusion is the controlling step (Fig. 6(e)). k_{id} is the intraparticle diffusion rate constant. A line that fails to pass through the origin would indicate some degree of film diffusion control, which would mean that intraparticle diffusion is not the only rate limiting step. The correlation coefficient ($R^2 > 0.9$) was in good agreement with the model parameters (Table 9) [28].

4.2.6. Avrami model

From the slope and intercept of the linear plot of (ln [–ln (1 – q_t/q_e)]) against ln t (Fig. 6(f)), the Avrami model parameters m_{Av} and k_{Av} were calculated to understand the influence of operational parameters (Table 9). The Avrami model values varied according to the nature of the coagulant used for treating the effluent. Irrespective of prevailing conditions, the m_{Av} value was greater than 1, and linear regression coefficient was above 0.9 [55,56].

The kinetics of pollutant binding onto a coagulant was substantiated by the Avrami model, which affirmed that the reaction was located on the surface active sites of the solid support. The m_{Av} values served to verify the effect of contact time on the adsorption mechanism, and also assisted in

Table 9
Kinetic model parameter values

Model parameters		*S. potatorum*	*C. opuntia*	*M. oleifera*	*C. tetragonolobus*	*P. sanguinolentus*
Pseudo-first order	R^2	0.900	0.977	0.914	0.942	0.951
	k'	0.048	0.037	0.044	0.035	0.055
	q_e(eqn)	301	144	191	108	191
	q_e(exp)	225	134	151	89	150
Elovich	R^2	0.985	0.976	0.989	0.993	0.955
	α_E	16	589	25	0.305	1001
	β_E	0.256	0.473	0.389	0.650	0.397
Intraparticle diffusion	R^2	0.925	0.977	0.942	0.892	0.973
	k_{id}	30.8	17.2	20.38	11.85	20.69
	I	–27.9	–8.8	–16.8	–14.3	–10.5
Bangham	R^2	0.983	0.999	0.996	0.975	0.986
	m_B	1.088	1.420	1.127	0.761	1.339
	k_B	5.470	7.379	4.188	0.460	7.621
Avrami	R^2	0.947	0.987	0.970	0.996	0.983
	m_{Av}	1.468	1.088	1.395	1.787	1.355
	$k_{Av} \times 10^{-5}$	0.968	20.8	1.71	0.0384	4.35

Table 10
Time growth of cluster size distribution per liter

Time (min)	0	10	20	30	40	50	60
S. potatorum							
Monomer particles count	457	166	85	52	35	25	19
Dimmer particles count	0	66	48	34	25	19	15
Trimmer particles count	0	26	27	13	18	15	12
Total particles count	457	258	161	109	78	58	45
C. opuntia							
Monomer particles count	457	272	181	129	96	75	60
Dimmer particles count	0	62	67	60	52	44	38
Trimmer particles count	0	14	25	28	28	26	24
Total particles count	457	349	273	217	176	146	122
M. oleifera							
Monomer particles count	457	138	65	38	25	17	13
Dimmer particles count	0	62	41	27	19	14	11
Trimmer particles count	0	28	25	19	15	11	9
Total particles count	457	228	131	84	58	43	33
C. tetragonolobus							
Monomer particles count	457	193	106	67	46	34	26
Dimmer particles count	0	68	55	41	31	25	20
Trimmer particles count	0	24	28	26	21	18	15
Total particles count	457	284	190	134	99	76	60
P. sanguinolentus							
Monomer particles count	457	160	81	49	32	23	17
Dimmer particles count	0	65	47	33	24	18	14
Trimmer particles count	0	27	27	22	17	14	11
Total particles count	457	252	155	104	74	55	43

quantifying the areas covered by heterogeneous reactions. The value also, made it possible to determine whether the adsorption process is limited by surface reaction ($m_{Av} > 1$) or not [57].

4.2.7. Cluster size distribution

The growth of aggregating particles as a function of time was evaluated for monomers (m = 1), dimmers (m = 2) and trimmers (m = 3), respectively, using Eq. (1). The curve trend is similar for all the coagulants. The number of monomer particles declined rapidly than the total number of particles. The least count of particles is viewed in the trimmer. The declined nature of monomer particles promoted the generation of the dimmer and trimmer particles. The number of monomer, dimmer, trimmer and total particle is listed in Table 10 and plotted in Figs. 7(a)–(e), for the green coagulants [34].

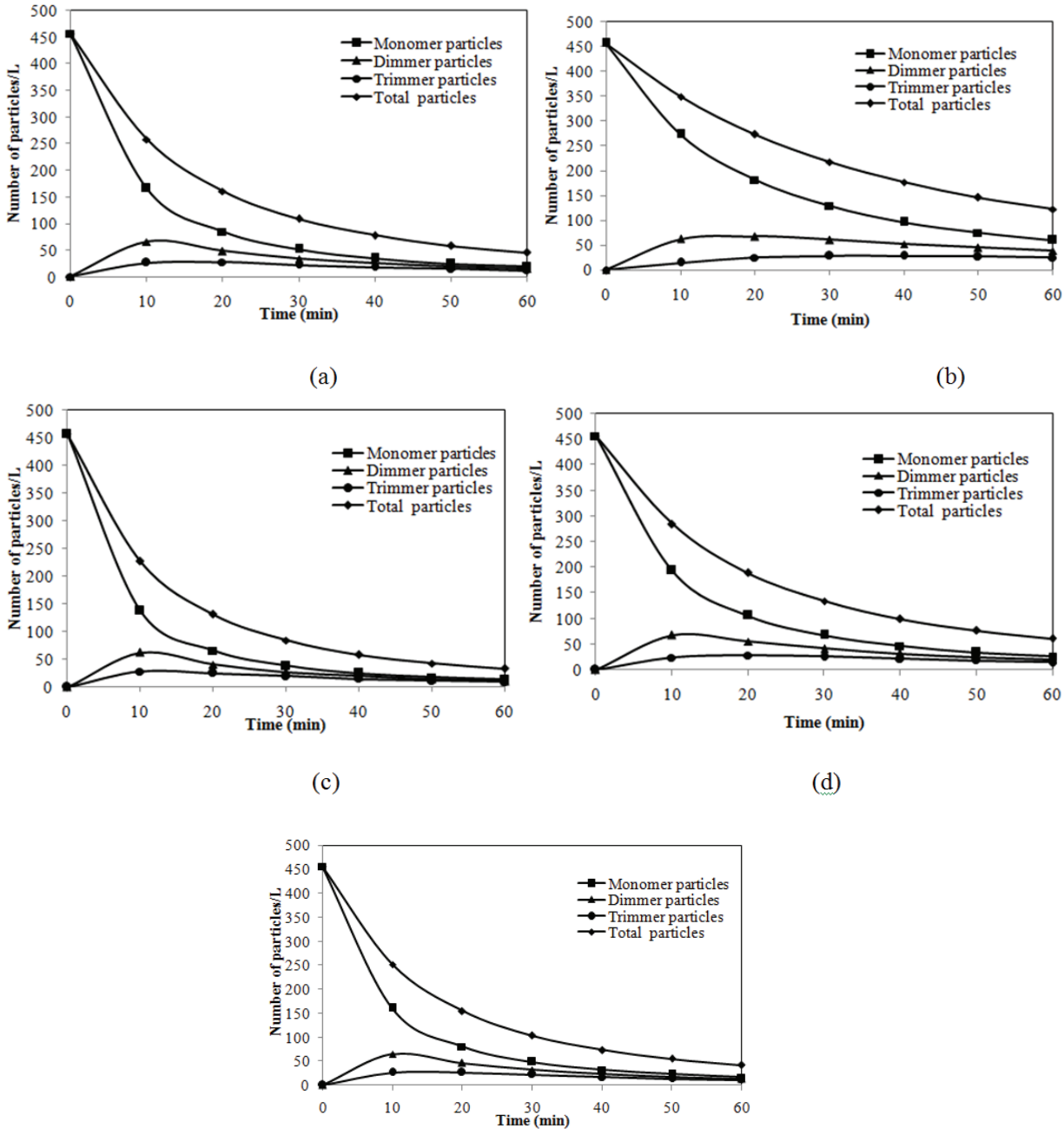

Fig. 7. Time evolution of the cluster size distribution. (a) *S. potatorum*, (b) *C. opuntia*, (c) *M. oleifera*, (d) *C. tetragonolobus* and (e) *P. sanguinolentus*.

5. Conclusions

The coagulation ability of the active component extracted from the natural and green coagulant viz, *S. potatorum* (proteins), *C. opuntia* (cellulose), *M. oleifera* (proteins), *C. tetragonolobus* (polysaccharides) and *P. sanguinolentus* (chitosan) was examined on SPE and RPE regarding color and turbidity. The removal efficiency has been found to be influenced by eluent type and concentration, coagulant dose, coagulant–eluate volume, initial effluent pH and initial effluent concentration and coagulation time. It was noticed that the treatment ability of the green coagulants is consistent in the RPE that of SPE. The coagulation kinetic behavior was established using various kinetic models. From the model parameters, it was demonstrated that the process followed a pseudo-first-order model. The fitness of the data with Elovich model reaffirms heterogeneity surface of coagulants and absence of chemisorption and Avrami model also supports this. The parameters of Bangham model and the larger linear regression values made it evident that the removal process was pore diffusion controlled. A line that fails to pass through the origin in the intraparticle diffusion model would indicate some degree of film diffusion control, which would mean that intraparticle diffusion is not the only rate limiting step. The cluster size distribution as a function of time revealed that the destabilization of the monomer particles enhances the formation of dimmer and trimmer particles.

This study suggested that being a biodegradable, abundance in nature; green coagulants could be the better surrogate for the chemical coagulants in the treatment of RPE.

Symbols

C_o, C_e, C_t	—	Concentration of the solute, at t = 0, at equilibrium and time t in the effluent, mg/L
D	—	Brownian diffusion coefficient, kg^2/m s
E	—	Collision efficiency
I	—	Thickness of boundary layer, mg/g
k_{Av}	—	Kinetic constant in the Avrami model
k_B	—	Kinetic constant in the Bangham model, mg/g min
$k_{Bo,}$	—	1,381 × 10^{-23} Boltzmann constant, m^2 kg/s^2 K
k_{id}	—	Kinetic rate constant in the intraparticle diffusion model, mg/g min$^{0.5}$
K_{Rc}	—	Smoluchowski rate constant for rapid coagulation, 1/min
k_1, k'	—	Kinetic rate constant in the first-order model, 1/min, pseudo-first order model, 1/min
m	—	Total mass of adsorbent, g
m_{Av}	—	Avrami model parameter
m_B	—	Bangham model parameter
N	—	Order of the coagulation process
N_o	—	Initial particle concentration, mg/L
q_t, q_e	—	Total quantity of pollutant adsorbed at time t and at equilibrium time, mg/g
$q_{e,exp}$, $q_{e,eqn}$	—	Equilibrium uptake of pollutants from the experiment and model equation, mg/g
R^2	—	Correlation coefficient
T	—	Absolute temperature, K
t	—	Coagulation process time, min
$t_{0.5}$	—	Time required for 50% removal of initial concentration, min
V	—	Volume of effluent, mL
α_E	—	Initial adsorption rate in the Elovich model, mg/mg
β	—	Friction factor due to shear stress, m^3/(kg s)
β_E	—	Desorption constant in the Elovich model, g/mg
μ	—	Effluent viscosity, kg m/s

References

[1] G. Srinivas, Industry Analysis Report on Paint Industry, Jawaharlal National Technical University, Hyderabad, India, 2010.
[2] www.virtusglobal.com.
[3] http://planningcommissiongovin/aboutus/committee.
[4] A. Akyol, Treatment of paint manufacturing wastewater by electrocoagulation, Desalination, 285 (2012) 91–99.
[5] C.P. Haung, M. Ghadirian, Physical–Chemical treatment of paint industry wastewater, J. Water Pollut. Control Fed., 46 (1974) 2340–2346.
[6] J.A. Brown, M. Weintraub, Bio oxidation of paint process wastewater, J. Water Pollut. Control Fed., 54 (1982) 1127–1131.
[7] M.C. Arquiaga, L.W. Canter, J.M. Robertson, Microbiological characterization of the biological treatment of aircraft paint stripping wastewater, Environ. Pollut., 89 (1995) 189–195.
[8] S. Shanta, S.N. Kaul, Performance of evaluation of a pure oxygen-based activated sludge system treatment a combined paint industry wastewater and domestic sewage, Int. J. Environ. Stud., 58 (2000) 445–457.
[9] B. Sengupta, B.K. Dey, M. Hashim, S. Hasan, Micro filtration of water-based paint effluents, Int. J. Environ. Manage., 8 (2004) 455–466.
[10] M.A. Aboulhassan, S. Souabi, A. Yaacoubi, M. Baudu, Improvement of paint effluents coagulation using natural and synthetic coagulant aids, J. Hazard. Mater., 138 (2006) 40–45.
[11] J.M. Xiang, L.X. Hui, Treatment of water based printing ink wastewater by Fenton process combined with coagulation, J. Hazard. Mater., 162 (2009) 386–390.
[12] M.Y. Pamukoglu, F. Kargi, Removal of copper (II) ions from aqueous medium by biosorption onto powdered waste sludge, Process Biochem., 41 (2006) 1047–1054.
[13] B.K. Korbahti, A. Tanyolac, Electrochemical treatment of simulated industrial paint wastewater in a continuous tubular reactor, Chem. Eng. J., 148 (2009) 444–445.
[14] A.E. Mohsen, H. Hassanin, M.M. Kamel, Appropriate technology for industrial wastewater treatment of paint industry, Am. Eurasian Agric. Environ., 8 (2010) 597–601.
[15] S. Gaurav, K. Anuj, M. Naushad, K. Amit, A.H.A. Muhtaseb, D. Pooja, A.G. Ayman, F.J. Stadler, M.R. Khan, Photoremediation of toxic dye from aqueous environment using monometallic and bimetallic quantum dots based nanocomposites, J. Clean. Prod., 172 (2018) 2919–2930.
[16] G. Sharma, M. Naushad, K. Amit, R. Shailja, S. Shweta, B. Amit, F.J. Stadler, A.G. Ayman, M. RizwanKhan, Efficient removal of coomassie brilliant blue R-250 dye using starch/poly(alginic acid-cl-acrylamide) nanohydrogel, Process Saf. Environ., 109 (2017) 301–310.
[17] P. Deepak, S. Gaurav, K. Amit, M. Naushad, K. Susheel, S. Anu, Z.A. Alothman, Combined sorptional–photocatalytic remediation of dyes by polyaniline Zr(IV) selenotungstophosphate nanocomposite, Toxicol. Environ. Chem., 97 (2015) 526–537.
[18] A.A. Alqadami, M. Naushad, M.A. Abdalla, M. Rizwan Khan, A.A. Zeid, Adsorptive removal of toxic dye using Fe_3O_4–TSC nanocomposite: equilibrium, kinetic, and thermodynamic studies, *J. Chem. Eng. Data*, 61 (2016) 3806–3813.
[19] P. Deepak, G. Divya, A.H.A. Muhtaseb, S. Gaurav, K. Amit, M. Naushad, A. Tansir, S.M. Alshehri, Photocatalytic degradation

of highly toxic dyes using chitosan-g-poly(acrylamide)/ZnS in presence of solar irradiation, J. Photochem. Photobiol., A., 329 (2016) 61–68.
[20] M. Naushad, Z.A. Alothman, M.R. Awual, S.M. Alfadul, A. Tansir, Adsorption of rose Bengal dye from aqueous solution by amberlite Ira-938 resin: kinetics, isotherms, and thermodynamic studies, Desal. Wat. Treat., 57 (2016) 13527–13533.
[21] T.P. Flaten, Aluminium as a risk factor in Alzheimer's disease, with emphasis on drinking water, Brain Res., 55 (2001) 187–196.
[22] R.M. Sudhir Dahiya, A.G. Tripathi, Hegde, Biosorption of lead and copper from aqueous solutions by pre-treated crab and arca shell biomass, Bioresour. Technol., 8 (2008) 179–187.
[23] Y.Y. Chun, Emerging usage of plant based coagulants for water and wastewater treatment, Process Biochem., 45 (2010) 1437–1444.
[24] V.A.K. Verma, R. Dash, P. Bhunia, A review on chemical coagulation/flocculation technologies for removal of colour from textile wastewaters, J. Environ. Manage., 93 (2012) 154–168.
[25] R. Babu, M. Chaudhri, Home water treatment by direct filtration with natural coagulant, J. Water Health., 3 (2005) 27–30.
[26] G. Muthuraman, S. Sasikala, Removal of turbidity from drinking water using natural coagulants, J. Ind. Eng. Chem., 20 (2013) 1727–1731.
[27] K. Jayaram, I.Y.L.N. Murthy, H. Lalhruaitluanga, M.N.V. Prasad, Biosorption of lead from aqueous solution by seed powder of *Strychnos potatorum* L., Colloid Surf, B., 71 (2009) 248–254.
[28] P. Senthil Kumar, C. Senthamarai, A.S.L. Sai Deepthi, R. Bharani, Adsorption isotherms, kinetics and mechanism of Pb (II) ions removal from aqueous solution using chemically modified agricultural waste, Can. J. Chem. Eng., 9999 (2013) 1–7.
[29] A. Diaz, N. Rincon, A. Escorihuela, N. Fernandez, E. Chacin, C.F. Forster, A preliminary evaluation of turbidity removal by natural coagulants indigenous to Venezuela, Process Biochem., 35 (1999) 391–395.
[30] U.S. Carpinteyro, M. Vaca, L. Torres, Can vegetal biopolymers work as coagulant-flocculant aids in the treatment of high-load cosmetic industrial wastewaters?, Water Air Soil Pollut., 223 (2012) 4925–4936.
[31] V.S. Adki, J.P. Jadhav, V.A. Bapat, Exploring the phytoremediation potential of cactus (*Nopalea cochenillifera Salm* Dyck) cell cultures for textile dye degradation, Int. J. Phytorem., 14 (2012) 554–569.
[32] E. Ikeda, D.G. Rodrigues, J. Nozaki, Treatment of effluents of poultry slaughterhouse with aluminum salts and natural polyelectrolytes, Environ. Technol., 23 (2002) 949–954.
[33] R. Kannan, S. Radha, N. Aparna, S. Vishali, W.R. Thilagaraj, Biosorption of heavy metals from actual electroplating wastewater using encapsulated *Moringa oleifera* beads in fixed bed column, Desal. Wat. Treat., 57 (2016) 3572–3587.
[34] M. Magesh kumar, R. Karthikeyan, Modeling the kinetics of coagulation process for tannery industry effluent treatment using *Moringa oleifera* seeds protein, Desal. Wat. Treat., 57 (2016) 14954–14964.
[35] L. Rizzo, A.D. Gennaro, M. Gallo, V. Belgiorno, Coagulation/chlorination of surface water: a comparison between chitosan and metal salts, Sep. Sci. Technol., 62 (2008) 79–85.
[36] S.G. Bhaskar, J.E. Ako, Application of guar gum as a flocculant aid in food processing and potable water treatment, Eur. Food Res. Technol., 221 (2005) 746–751.
[37] B. Saritha, G. Sharmilaa, Treatability study of tannery effluent by using guar gum with coagulants alum and ferric sulphate, Int. J. Eng. Trends Technol., 2 (2011) 1–7.
[38] B. Saritha, G. Sharmilaa, Study of removal of COD by guar gum with coagulants alum and polyaluminium chloride in wastewater treatment, Int. J. Bio. Trends Technol., 2 (2012) 11–19.
[39] L. Shuguang, S.W. Gibb, E. Cochrane, Effective removal of zinc ions from aqueous solutions using crab carapace biosorbent, J. Hazard. Mater., 149 (2007) 208–217.
[40] H. Zemmouri, M. Drouiche, A. Sayeh, H. Lounici, N. Mameri, Coagulation flocculation test of keddara's water dam using chitosan and sulfate aluminum, Procedia Eng., 33 (2012) 254–260.
[41] F. H. Chi, W.P. Cheng, Use of chitosan as coagulant to treat wastewater from milk processing plant, J. Polym. Environ., 14 (2006) 411–417.
[42] Y. Bolat, S. Bilgin, A. Gunlu, L. Izci, S.B. Koca, S. Cetinkaya, H.U. Koca, Chitin-chitosan yield of freshwater crab (*Potamon potamios,* Olivier 1804) shell, Pak. Vet. J., 30 (2010) 227–231.
[43] K.K. Bahadir, A. Tanyolac, Electrochemical treatment of simulated industrial paint wastewater in a continuous tubular reactor, Chem. Eng. J., 148 (2009) 444–451.
[44] APHA, Standard Methods for the Examination of Waste and Wastewater, 16th edition, American Public Health Associations, New York, NY, 1995.
[45] M.A. Hossain, H.H. Ngo, W.S. Guo, T.V. Nguyen, Palm oil fruit shells as biosorbent for copper removal from water and wastewater: experiments and sorption models, Bioresour. Technol., 113 (2012) 97–101.
[46] M. Akhtara, S. Iqbal, M.T. Bhanger, Z.U.M. Haqc, M.M. Moazzamd, Sorption of organo phosphorous pesticides onto chickpea husk from aqueous solutions, Colloid Surf. B, 69 (2009) 63–70.
[47] A. Sari, D. Mendil, M. Tuzen, M. Soylak, Biosorption of Cd(II) and Cr(III) from aqueous solution by moss (*Hylocomium splendens*) biomass: equilibrium, kinetic and thermodynamic studies, Chem. Eng. J., 144 (2008) 1–9.
[48] E. Repo, EDTA- and DTPA-Functionalized Silica Gel and Chitosan Adsorbents for the Removal of Heavy Metals from Aqueous Solutions, Dissertation, Lappeenranta University of technology, Finland, 2011.
[49] A. Rathinam, B. Maharshi, S.K. Janardhanan, R.R. Jonnalagadda, B.U. Nair, Biosorption of cadmium metal ion from simulated wastewaters using *Hypnea valentiae* biomass: a kinetic and thermodynamic study, Bioresour. Technol., 101 (2010) 1466–1470.
[50] S. Vishali, R. Karthikeyan, A comparative study of *Strychnos potatorum* and chemical coagulants in the treatment of paint and industrial effluents: an alternate solution, Sep. Sci. Technol., 49 (2014) 2510–2517.
[51] S. Vishali, R. Karthikeyan, *Cactus opuntia (ficus-indica):* an eco-friendly alternative coagulant in the treatment of paint effluent, Desal. Wat. Treat., 56 (2015) 1489–1497.
[52] S. Vishali, P. Rashmi, R. Karthikeyan, Evaluation of wasted biomaterial, crab shells *(Portunus sanguinolentus*), as a coagulant, in paint effluent treatment, Desal. Wat. Treat., 57 (2016) 13157–13165.
[53] S. Vishali, A. Ayushi, Performance evaluation of *Cyamopsis tetragonolobus* (guar gum), as a natural coagulant, in the treatment of paint industry effluent, Desal. Wat. Treat., 62 (2017) 443–448.
[54] E. Bulut, M. Ozacar, I. Ayhan, S. Engil, Adsorption of malachite green onto bentonite: equilibrium and kinetic studies and process design, Microporous Mesoporous Mater., 115 (2008) 234–246.
[55] R. Nadeem, M.H. Nasir, M.S. Hanif, Pb (II) sorption by acidically modified *Cicer arientinum* biomass, Chem. Eng. J., 150 (2009) 40–48.
[56] K. Ada, A. Ergene, S. Tan, E. Yal, Adsorption of Remazol Brilliant Blue R using ZnO fine powder: equilibrium, kinetic and thermodynamic modeling studies, J. Hazard. Mater., 165 (2009) 637–644.
[57] R. George, S. Sugunan, Kinetics of adsorption of lipase onto different mesoporous materials: evaluation of Avrami model and leaching studies, J. Mol. Catal. B Enzym., 105 (2014) 26–32.